

# Neutrino Interaction Calculations from MeV to GeV Region

J.E. Amaro\*, J. Nieves\*, M. Valverde\* and M.J. Vicente-Vacas†

*\*Departamento de Física Atómica, Molecular y Nuclear,  
Universidad de Granada, E-18071 Granada, Spain*

*†Departamento de Física Teórica and IFIC, Centro Mixto Universidad de Valencia-CSIC  
Institutos de Investigación de Paterna, Aptdo. 22085, E-46071 Valencia, Spain*

**Abstract.** The Quasi-Elastic (QE) contribution of the nuclear inclusive electron model developed in reference [1] is extended to the study of neutrino/antineutrino Charged Current (CC) and Neutral Current (NC) induced nuclear reactions at intermediate energies. Long range nuclear (RPA) correlations, Final State Interaction (FSI) and Coulomb corrections are included within the model. RPA correlations are shown to play a crucial role in the whole range (100–500 MeV) of studied neutrino energies. Results for inclusive muon capture for different nuclei through the Periodic Table are also discussed. In addition, and by means of a Monte Carlo cascade method to account for the rescattering of the outgoing nucleon, we also study the CC and NC inclusive one nucleon knockout reactions off nuclei.

**Keywords:** neutrino induced nuclear reactions

**PACS:** 25.30.Pt, 13.15.+g, 24.10.Cn, 21.60.Jz

## INTRODUCTION

Neutrino physics is at the forefront of current theoretical and experimental research in astro, nuclear, and particle physics. Indeed, neutrino interactions offer unique opportunities for exploring fundamental questions in these domains of the physics. One of these questions is the neutrino-oscillation phenomenon, for which there have been conclusive positive signals in the last years [2]. The presence of neutrinos, being chargeless particles, can only be inferred by detecting the secondary particles they create when colliding and interacting with matter. Nuclei are often used as neutrino detectors, thus a trustable interpretation of neutrino data heavily relies on detailed and quantitative knowledge of the features of the neutrino-nucleus interaction. There is a general consensus among the theorists that a simple Fermi Gas (FG) model, widely used in the analysis of neutrino oscillation experiments, fails to provide a satisfactory description of the measured cross sections, and inclusion of further nuclear effects is needed [3].

Any model aiming at describing the interaction of neutrinos with nuclei should be firstly tested against the existing data on the interaction of real and virtual photons with nuclei. For nuclear excitation energies ranging from about 100 MeV to 500 or 600 MeV, three different contributions should be taken into account: i) QE processes, ii) pion production and two body processes from the QE region to that beyond the  $\Delta(1232)$  resonance peak, and iii) double pion production and higher nucleon resonance degrees of freedom induced processes. The model developed in Refs. [1] (inclusive electro-nuclear reactions) and [4] (inclusive photo-nuclear reac-

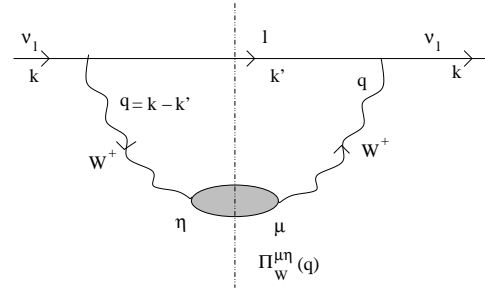


**FIGURE 1.** Diagrammatic representation of the neutrino selfenergy in nuclear matter.

tions) has been successfully compared with data at intermediate energies and it systematically includes the three type of contributions mentioned above. Nuclear effects are computed starting from a local FG picture of the nucleus, an accurate approximation to deal with inclusive processes which explore the whole nuclear volume [4], and their main features, expansion parameter and all sort of constants are completely fixed from previous hadron-nucleus studies (pionic atoms, elastic and inelastic pion-nucleus reactions,  $\Lambda$ -hypernuclei, etc...) [5, 6]. Thus, and besides the photon coupling constants determined in the vacuum, the model of Refs. [1] and [4] has no free parameters, and thus the results presented in these two references are predictions deduced from the nuclear microscopic framework developed in Refs. [5] and [6]. In this talk, we extend the nuclear inclusive QE electron scattering model of Ref. [1], including the axial CC [7] and NC [8] degrees of freedom, to describe neutrino and antineutrino induced nuclear reactions in the QE region.

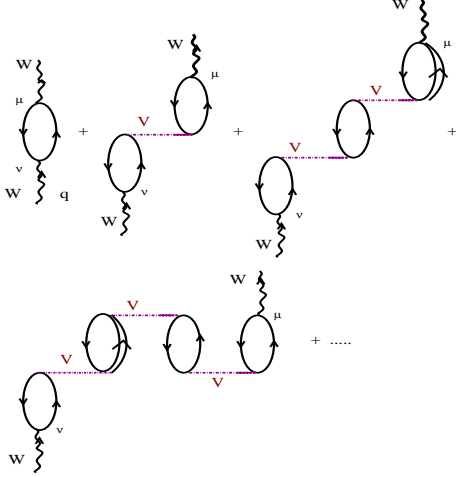


**FIGURE 2.** Set of irreducible diagrams responsible for the polarization (RPA) effects in the 1p1h contribution to the  $W$ -selfenergy.

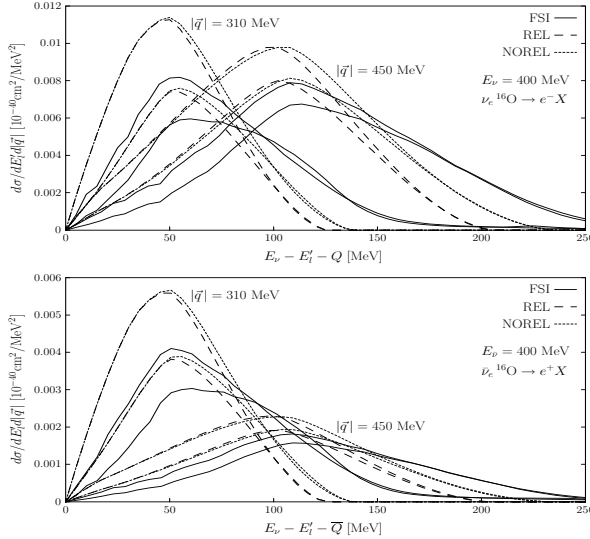


**FIGURE 3.**  $\nu_e$ – (top) and  $\bar{\nu}_e$ – (bottom) inclusive QE differential cross sections in oxygen as a function of the transferred energy, at two values of the transferred momentum. We show results for relativistic (REL) and non-relativistic nucleon kinematics. In this latter case, we present results with (FSI) and without (NOREL) FSI effects. For the three cases, we also show the effect of taking into account RPA correlations and Coulomb corrections (lower lines at the peak).

We also present results for the QE ( $\nu_l, \nu_l N$ ), ( $\nu_l, l^- N$ ), ( $\bar{\nu}_l, \bar{\nu}_l N$ ) and ( $\bar{\nu}_l, l^+ N$ ) reactions in nuclei. We use a Monte Carlo (MC) simulation method to account for the rescattering of the outgoing nucleon. The first step is the gauge boson ( $W^\pm$  and  $Z^0$ ) absorption in the nucleus. We take this reaction probability from the microscopical

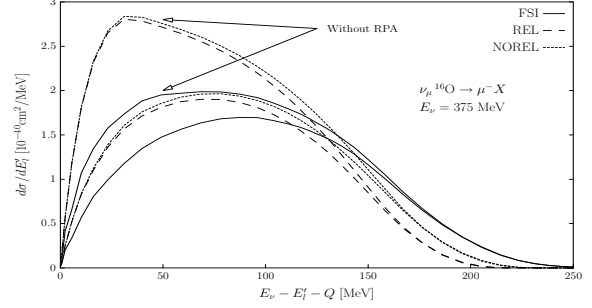


**FIGURE 4.** Muon neutrino inclusive QE differential cross sections in oxygen as a function of the transferred energy. The notation for the theoretical predictions is the same as in Fig. 3.

many body framework developed in Refs. [7, 8] for CC and NC induced reactions. Some calculations found in the literature use the plane wave and distorted wave impulse approximations (PWIA and DWIA, respectively), including or not relativistic effects. The PWIA constitutes a poor approximation, since it neglects all types of interactions between the ejected nucleon and the residual nuclear system. The DWIA describes the ejected nucleon as a solution of the Dirac or Schrödinger equation with an optical potential obtained by fitting elastic proton–nucleus scattering data. The imaginary part accounts for the absorption into unobserved channels. This scheme is incorrect to study nucleon emission processes where the state of the final nucleus is totally unobserved, and thus all final nuclear configurations, either in the discrete or on the continuum, contribute. The distortion of the nucleon wave function by a complex optical potential removes all events where the nucleons collide inelastically with other nucleons. Thus, in DWIA calculations, the nucleons that interact inelastically are lost when in the physical process they simply come off the nucleus with a different energy, angle, and maybe charge, and they should definitely be taken into account. A clear example which illustrates the deficiencies of the DWIA models is the neutron emission process: ( $\nu_l, l^- n$ ). Within the impulse approximation neutrinos only interact via CC interactions with neutrons and would emit protons, and therefore the DWIA will predict zero cross sections for CC one neutron knock-out reactions. However, the primary protons interact strongly with the medium and collide with other nucleons which are also ejected. As a consequence there is a reduction of the flux of high energy protons but a large number of secondary nucleons, many of them neutrons, of lower energies appear.

Finally, we would like to mention that we have already started working on one and two pion production processes in nuclei, aiming to extend the present study beyond the QE peak to the  $\Delta(1232)$  resonance region. As a first step, we have studied the production off the

nucleon [9, 10] and some results have been also reported at this conference [11].

## INCLUSIVE QE CROSS SECTIONS

We will expose here the general formalism focusing on the neutrino CC reaction. The generalization to antineutrino CC, neutrino and antineutrino NC reactions or inclusive muon capture is straightforward. In the laboratory frame, the differential cross section for the process  $\nu_l(k) + A_Z \rightarrow l^-(k') + X$  reads:

$$\frac{d^2\sigma}{d\Omega(\hat{k}')dE_l'} = \frac{|\vec{k}'|}{|\vec{k}|} \frac{G^2}{4\pi^2} L_{\mu\sigma} W^{\mu\sigma} \quad (1)$$

with  $L$  and  $W$  the leptonic and hadronic tensors, respectively. On the other hand, the inclusive CC nuclear cross section is related to the imaginary part of the neutrino self-energy (see Fig. 1) in the medium by:

$$\sigma = -\frac{1}{|\vec{k}|} \int \text{Im}\Sigma_\nu(k; \rho(r)) d^3r \quad (2)$$

We obtain the imaginary part of the neutrino self-energy in the medium,  $\text{Im}\Sigma_\nu$ , by means of the Cutkosky's rules: in this case we cut with a vertical straight line (see Fig. 1) the intermediate lepton state and those implied by the  $W$ -boson medium self-energy. Those states are placed on shell by taking the imaginary part of the propagator, self-energy, etc. We obtain for  $k^0 > 0$

$$\text{Im}\Sigma_\nu(k) = \frac{8G\Theta(q^0)}{\sqrt{2}M_W^2} \int \frac{d^3k'}{(2\pi)^3} \frac{\text{Im}\{\Pi_W^{\mu\eta} L_{\eta\mu}\}}{2E_l'} \quad (3)$$

and thus, the hadronic tensor is basically an integral over the nuclear volume of the  $W$ -selfenergy ( $\Pi_W^{\mu\nu}(q; \rho)$ ) inside the nuclear medium. We can then take into account the different in-medium effects and reaction mechanism modes ( $W$  absorption by one nucleon or by a pair of nucleons, pion production, excitation of resonances,...) by including the correspondent diagrams in the  $W$ -selfenergy (shaded loop of Fig. 1). Further details can be found in Refs. [1, 7].

The virtual  $W$  gauge boson can be absorbed by one nucleon, 1p1h nuclear excitation, leading to the QE contribution to the nuclear response function. We consider a structure of the  $V-A$  type for the  $W^+pn$  vertex, and use PCAC and invariance under G-parity to relate the pseudoscalar form factor to the axial one and to discard a term of the form  $(p^\mu + p'^\mu)\gamma_5$  in the axial sector, respectively. Besides, and thanks to isospin symmetry, the vector form factors are related to the electromagnetic ones. We find

$$W^{\mu\nu}(q) = \frac{\cos^2\theta_C}{2M^2} \int_0^\infty dr r^2 \left\{ \Theta(q^0) \int \frac{d^3p}{4\pi^2} \frac{M}{E(\vec{p})} \right.$$

$$\left. \frac{M}{E(\vec{p}+\vec{q})} \Theta(k_F^n(r) - |\vec{p}|) \Theta(|\vec{p}+\vec{q}| - k_F^p(r)) \delta(q^0 + E(\vec{p}) - E(\vec{p}+\vec{q})) A^{\nu\mu}(p, q)|_{p^0=E(\vec{p})} \right\} \quad (4)$$

with the local Fermi momentum  $k_F(r) = (3\pi^2\rho(r)/2)^{1/3}$ ,  $M$  the nucleon mass, and  $E(\vec{p}) = \sqrt{M^2 + \vec{p}^2}$ . We work on a non-symmetric nuclear matter with different Fermi sea levels for protons,  $k_F^p$ , than for neutrons,  $k_F^n$  (equation above, but replacing  $\rho/2$  by  $\rho_p$  or  $\rho_n$ , with  $\rho = \rho_p + \rho_n$ ). Finally,  $A^{\mu\nu}$  is the CC nucleon tensor [7] and is determined by the  $W^+pn$  form-factors. The  $d^3p$  integrations above can be done analytically and all of them are determined by the imaginary part of isospin asymmetric Lindhard function,  $\bar{U}(q, k_F^n, k_F^p)$ . Explicit expressions can be found in [7], where also antineutrino induced CC cross sections and the inclusive muon capture process in nuclei are discussed. Expressions for the NC hadron tensor can be found in Ref. [8].

## Nuclear Corrections

We take into account polarization effects by substituting the particle-hole (1p1h) response by an RPA response consisting of a series of ph and  $\Delta$ -h excitations, as shown in Fig. 2. We use an effective Landau-Migdal ph-ph interaction [12]:  $V = c_0 \{f_0 + f'_0 \vec{\tau}_1 \vec{\tau}_2 + g_0 \vec{\sigma}_1 \vec{\sigma}_2 + g'_0 \vec{\sigma}_1 \vec{\tau}_1 \vec{\tau}_2\}$ . In the vector-isovector channel ( $\vec{\sigma} \vec{\sigma} \vec{\tau} \vec{\tau}$  operator) we use an interaction [1, 4, 6] with explicit  $\pi$ -meson (longitudinal) and  $\rho$ -meson (transverse) exchanges, and that also includes  $\Delta(1232)$  degrees of freedom. This effective interaction is non-relativistic, and then for consistency we will neglect terms of order  $\mathcal{O}(p^2/M^2)$  when summing up the RPA series.

We also ensure the correct energy balance of the different studied processes by modifying the energy conserving  $\delta$  function in Eq. (4) to account for the experimental  $Q$ -value of the reaction. Besides, we consider the effect of the Coulomb field of the nucleus acting on the ejected charged lepton, as well. This is done by including the lepton self-energy  $\Sigma_C = 2k'^0 V_C(r)$  in the intermediate lepton propagator of Fig. 1.

Finally, we take into account the modification of nucleon dispersion relation in the medium (FSI) by using nucleon propagators properly dressed with a realistic self-energy. We use a dynamical model in which the nucleon self-energy depends explicitly on the energy and the momentum [13]. Thus, we compute the imaginary part of the Lindhard function (ph propagator) using realistic spectral functions  $S_{p,h}(\omega, \vec{p}; \rho)$ .

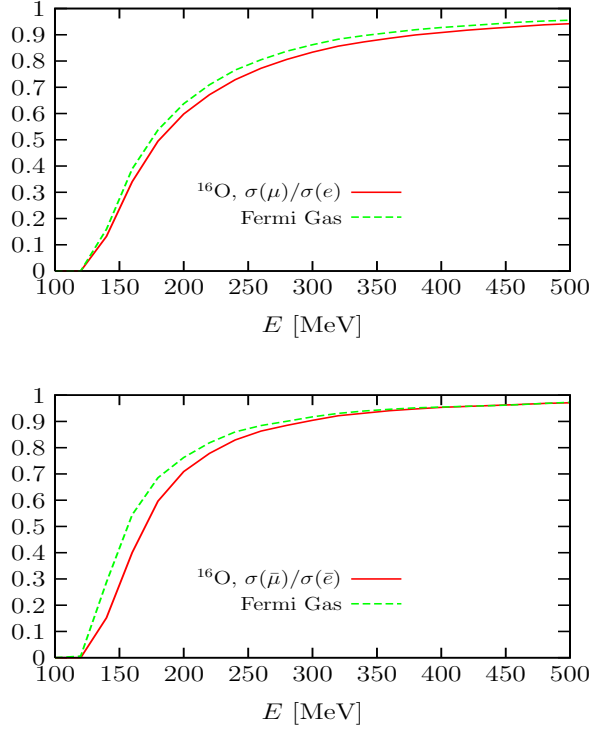


**FIGURE 5.** Ratio of inclusive QE cross sections induce by neutrinos (top) and antineutrinos (bottom) in oxygen, as a function of the incoming neutrino energy. Solid and dashed lines stand for the predictions of the model of Ref. [7] and from the FG model, respectively.

## CC AND NC INCLUSIVE ONE NUCLEON KNOCKOUT REACTIONS

We use a cascade method to account for the rescattering of the outgoing nucleon. The first step is the gauge boson ( $W^\pm$  and  $Z^0$ ) absorption in the nucleus, we take this reaction probability from the microscopical many body framework outlined in the previous section for CC and NC induced reactions. It is given by the inclusive QE cross sections  $d^2\sigma/d\Omega'dE'$  ( $\Omega'$ ,  $E'$  are the solid angle and energy of the outgoing lepton) for a fixed incoming neutrino or antineutrino laboratory energy. We also compute differential cross sections with respect to  $d^3r$ . Thus, we also know the point of the nucleus where the gauge boson was absorbed, and we can start from there our MC propagation of the ejected nucleon. After the absorption of the gauge boson, we follow the path of the ejected nucleon through its way out of the nucleus using a MC simulation to account for the secondary collisions. Details on the MC simulation can be found in [8]. This MC simulator has been tested in different physical situations. It was first designed for single and multiple nucleon and pion emission reactions induced by pions [14, 15] and has been successfully employed to describe inclusive  $(\gamma, \pi)$ ,

$(\gamma, N)$ ,  $(\gamma, NN)$ , ...,  $(\gamma, N\pi)$ , ... [16, 17],  $(e, e'\pi)$ ,  $(e, e'N)$ ,  $(e, e'NN)$ , ...,  $(e, e'N\pi)$ , ... [18] reactions in nuclei or the neutron and proton spectra from the decay of  $\Lambda$  hypernuclei [19].

## RESULTS

### Inclusive cross sections

At low energies, the model provides a reasonable description of the LSND measurement of the reaction  $^{12}\text{C}(\nu_\mu, \mu^-)X$  near threshold, and of the accurate nuclear inclusive muon capture rates through the whole Periodic Table. Pauli blocking and the use of the correct energy balance provide the bulk of the corrections, but an accurate description of data is only achieved once the RPA correlations, including  $\Delta h$  excitations, are taken into account. Our approach provides one of the best existing combined descriptions of the inclusive muon capture in  $^{12}\text{C}$  and the LSND measurement of the reaction  $^{12}\text{C}(\nu_\mu, \mu^-)X$  near threshold [7], and certainly comparable to that achieved by other models, which implement a more sophisticated treatment of the dynamics of finite nuclei (see for instance the discussion in [20]).

At intermediate energies the predictions of our model become reliable not only for integrated, but also for differential cross sections. We present results for incoming neutrino energies within the interval 150-500 MeV for electron and muon species (some results at higher energies can be found in [21]). In Figs. 3 and 4, RPA and FSI effects on differential cross section are shown. RPA effects are extremely important in this range of energies and induce important corrections to the simple FG description. On the other hand, FSI provides a broadening and a significant reduction of the strength of the QE peak. Nevertheless the integrated cross section is only slightly modified. Though FSI change importantly the shape of the differential cross sections, it plays a minor role for totally integrated cross sections. When medium polarization effects are not considered, FSI provides significant reductions (15-30%) of the cross sections. However, when RPA corrections are included the reductions becomes more moderate, always smaller than 7%, and even there exist some cases where FSI enhances the cross sections. This can be easily understood by looking at Fig. 4. There, we see that FSI increases the cross section at high energy transfers. But for nuclear excitation energies higher than those around the QE peak, the RPA corrections are certainly less important than in the peak region. Thus, the RPA suppression of the FSI distribution is significantly smaller than the RPA reduction of the distribution determined by the ordinary Lindhard function.

We have estimated the theoretical uncertainties of our

model by MC propagating the uncertainties of its different inputs into differential and total cross sections [22]. We conclude that our approach provides QE  $\nu(\bar{\nu})$ -nucleus cross sections with relative errors of about 10-15%, while uncertainties affecting the ratios  $\sigma(\mu)/\sigma(e)$  and  $\sigma(\bar{\mu})/\sigma(\bar{e})$  would be certainly smaller, not larger than about 5%, and mostly coming from deficiencies of the local FG picture of the nucleus [22]. Though nuclear corrections cancel importantly in these ratios, there still exist some effects (Fig. 5).

## Nucleon Emission Reactions

CC and NC nucleon emission processes play an important role in the analysis of oscillation experiments. In particular, they constitute the unique signal for NC neutrino driven reactions. Different distributions for both NC and CC processes can be found in [8], as example, we show here results for NC nucleon emission from argon (Fig. 6). The rescattering of the outgoing nucleon produces a depletion of the high energy side of the spectrum, but the scattered nucleons clearly enhance the low energy region. Our results compare well with those of Refs. [23, 24] obtained by means of a transport model.

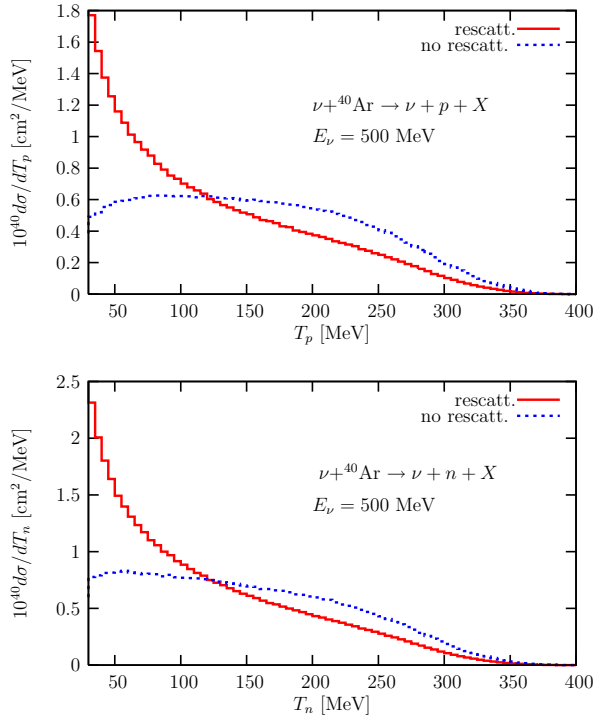


**FIGURE 6.** Neutral current  $^{40}\text{Ar}(\nu, \nu + N)$  at 500 MeV cross sections as a function of the kinetic energy of the final nucleon. The dashed histograms show results without rescattering (PWIA) and the solid ones have been obtained from the MC cascade simulation.

## ACKNOWLEDGMENTS

This work was partially supported by MEC contracts FIS2005-00810, FIS2006-03438, by the Generalitat Valenciana and by Junta de Andalucía under contracts ACOMP07/302 and FQM0225, and by the EU under contract RII3-CT-2004-506078.

## REFERENCES

1. A. Gil, J. Nieves and E. Oset, *Nucl. Phys.* **A627** 543 (1997).
2. Super-Kamiokande Collaboration, Y. Fukuda et al., *Phys. Rev. Lett.* **81** 1562 (1998); The K2K Collaboration, M. Ahn et al., *Phys. Rev. Lett.* **90** 041801 (2003).
3. O. Benhar, et al., *Phys. Rev.* **D72** 053005 (2005).
4. R.C. Carrasco and E. Oset, *Nucl. Phys.* **A536** 445 (1992).
5. E. Oset, H. Toki and W. Weise, *Phys. Rep.* **83** (1982) 281.
6. J. Nieves, E. Oset, C. García-Recio, *Nucl. Phys.* **A554** 509 (1993); *ibidem Nucl. Phys.* **A554** 554 (1993); C. Albertus, J.E. Amaro and J. Nieves, *Phys. Rev. Lett.* **89** (2002) 032501; *ibidem Phys. Rev.* **C67** (2003) 034604. C. García-Recio, J. Nieves, T. Inoue and E. Oset, *Phys. Lett.* **B550** 47 (2002).
7. J. Nieves, J.E. Amaro and M. Valverde, *Phys. Rev.* **C70** 055503 (2004); *Erratum-ibid* **C72**, 019902 (2005).
8. J. Nieves, M. Valverde and M.J. Vicente Vacas, *Phys. Rev.* **C73** 025504 (2006).
9. E. Hernández, J. Nieves and M. Valverde, *Phys. Rev.* **D76** 033005 (2007); *ibidem Phys. Lett.* **B647** 452 (2007).
10. E. Hernández, J. Nieves, S.K. Singh, M. Valverde and M.J. Vicente-Vacas, *arXiv:0710:3562 [hep-ph]*
11. E. Hernández, J. Nieves and M. Valverde, *arXiv:0710:5587 [hep-ex]*
12. J. Speth, E. Werner and W. Wild, *Phys. Rep.* **33** 127 (1977); J. Speth, V. Klemm, J. Wambach and G.E. Brown *Nucl. Phys.* **A343** 382 (1980).
13. P. Fernández de Córdoba and E. Oset, *Phys. Rev.* **C46** 1697 (1992).
14. L.L. Salcedo, E. Oset, M.J. Vicente Vacas and C. García Recio, *Nucl. Phys.* **A484** 557 (1988).
15. M. J. Vicente Vacas and E. Oset, *Nucl. Phys.* **A568** 855 (1994).
16. R.C. Carrasco, E. Oset and L.L. Salcedo, *Nucl. Phys.* **A541** 585 (1992).
17. R.C. Carrasco, M.J. Vicente-Vacas and E. Oset, *Nucl. Phys.* **A570** 701 (1994).
18. A. Gil, J. Nieves and E. Oset, *Nucl. Phys.* **A627** 599 (1997).
19. A. Ramos, M. J. Vicente Vacas and E. Oset, *Phys. Rev.* **C55** 735 (1997). *Erratum-ibid* **C66** 039903 (2002).
20. E. Kolbe, K. Langanke, G. Martínez-Pinedo and P. Vogel, *J. Phys.* **G29** 2569 (2003).
21. M. S. Athar, S. Ahmad and S. K. Singh, *Phys. Rev.* **D75** 093003 (2007).
22. M. Valverde, J.E. Amaro and J. Nieves, *Phys. Lett.* **B638** 325 (2006).
23. O. Buss, T. Leitner, U. Mosel and L. Alvarez-Ruso, *Phys. Rev.* **C76** 035502 (2007).
24. T. Leitner, L. Alvarez-Ruso and U. Mosel, *Phys. Rev.* **C74** 065502 (2006); *ibidem Phys. Rev.* **C73** 065502 (2006).